PO Box 2345, Beijing 100023, China
www.wjgnet.com
wjg@wjgnet.com

World J Gastroenterol 2006 March 28; 12(12): 1881-1888
World Journal of Gastroenterology ISSN 1007-9327

BASIC RESEARCH

Reconstruction of liver organoid using a bioreactor

Masaya Saito, Tomokazu Matsuura, Takahiro Masaki, Haruka Maehashi, Keiko Shimizu, Yoshiaki Hataba, Tohru Iwahori, Tetsuro Suzuki, Filip Braet

Masaya Saito, Division of Gastroenterology and Hepatology, Department of Internal Medicine, The Jikei University School of Medicine, Tokyo, Japan
Tomokazu Matsuura, Department of Laboratory Medicine, The Jikei University School of Medicine, Tokyo, Japan
Takahiro Masaki, Tetsuro Suzuki, Department of Virology II, National Institute of Infectious Disease, Tokyo, Japan
Haruka Maehashi, Keiko Shimizu, First Department of Biochemistry, The Jikei University School of Medicine, Tokyo, Japan
Yoshiaki Hataba, DNA Medical Institute, The Jikei University School of Medicine, Tokyo, Japan
Tohru Iwahori, Fifth Division of Blood Purification, Department of Surgery, Tokyo Medical University, Tokyo, Japan
Filip Braet, Australian Key Center for Microscopy & Microanalysis, Electron Microscope Unit, The University of Sydney, NSW 2006, Australia
Supported by grants-in-aid from the University Start-Up Creation Support System, the Promotion and Mutual Aid Corporation for Private Schools of Japan, and The Japan Health Sciences Foundation (Research on Health Sciences on Drug Innovation, KH71068)
Correspondence to: Tomokazu Matsuura, MD, PhD, Department of Laboratory Medicine, The Jikei University School of Medicine, 3-25-8 Nishi-shinbashi, Minato-ku,
Tokyo 105-8461, Japan. matsuurat@jikei.ac.jp
Telephone: +81-3-34331111-3210 Fax: +81-3-34350569
Received: 2005-09-12 Accepted: 2005-10-26

Abstract

AIM: To develop the effective technology for reconstruction of a liver organ *in vitro* using a bio-artificial liver.

METHODS: We previously reported that a radial-flow bioreactor (RFB) could provide a three-dimensional high-density culture system. We presently reconstructed the liver organoid using a functional human hepatocellular carcinoma cell line (FLC-5) as hepatocytes together with mouse immortalized sinusoidal endothelial cell (SEC) line M1 and mouse immortalized hepatic stellate cell (HSC) line A7 as non parenchymal cells in the RFB. Two x 10^7 FLC-5 cells were incubated in the RFB. After 5 d, 2 x 10^7 A7 cells were added in a similar manner followed by another addition of 10^7 M1 cells 5 d later. After three days of perfusion, some cellulose beads with the adherent cells were harvested. The last incubation period included perfusion with 200 nmol/L swinholide A for 2 h and then the remaining cellulose beads along with adherent cells were harvested from the RFB. The cell morphology was observed by transmission electron microscopy (TEM) and scanning electron microscopy (SEM). To assess hepatocyte function, we compared mRNA expression for urea cycle enzymes as well as albumin synthesis by FLC-5 in monolayer cultures compared to those of single-type cultures and cocultures in the RFB.

RESULTS: By transmission electron microscopy, FLC-5, M1, and A7 were arranged in relation to the perfusion side in a liver-like organization. Structures resembling bile canaliculi were seen between FCL-5 cells. Scanning electron microscopy demonstrated fenestrae on SEC surfaces. The number of vesiculo-vacuolar organelles (VVO) and fenestrae increased when we introduced the actin-binding agent swinholide-A in the RFB for 2h. With respect to liver function, urea was found in the medium, and expression of mRNAs encoding arginosuccinate synthetase and arginase increased when the three cell types were cocultured in the RFB. However, albumin synthesis decreased.

CONCLUSION: Co-culture in the RFB system can dramatically change the structure and function of all cell types, including the functional characteristics of hepatocytes. Our system proves effective for reconstruction of a liver organoid using a bio-artificial liver.

Key words: Liver organoid; Organ reconstruction; Bio-artificial liver; Coculture; Liver sinusoidal endothelial cell; Hepatocytes; Fenestrae; Vesiculo vacuolar organelles; Radial flow bioreactor

Saito M, Matsuura T, Masaki T, Maehashi H, Shimizu K, Hataba Y, Iwahori T, Suzuki T, Braet F. Reconstruction of liver organoid using a bioreactor. *World J Gastroenterol* 2006; 12(12): 1881-1888

http://www.wjgnet.com/1007-9327/12/1881.asp

INTRODUCTION

Liver regeneration technology has made many advances in recent years. Efforts now are being made toward development of embryonic stem cells (ES cells), differentiation of hemopoietic stem cells, and development of isolation and culture methods for somatic stem cells originating from different organs. Hemopoietic stem cells, hepatoblasts originating from fetal liver, hepatocytes, and pancreatic duct epithelial cells have been included in the list of candi-

date cells for liver regeneration[1]. Development of immortalized cells by introduction of the simian virus 40 (SV40) large T antigen gene or human telomerase reverse transcriptase (hTERT) is also under investigation[2]. To date, however, no technique for regenerating and reconstructing parenchymal organs using these cells has been established. Conventional cell culture methods have achieved this goal clinically for skin, cornea, and bone tissue[3,4].

Reconstruction of organs such as the liver requires maintenance of viable cells at a high density and coculture under conditions favorable to several different cell types that constitute a liver. To make a culture system is important in reconstructing a liver organoid. Conventional stationary culture techniques are not well suited to the culture of cells in a layered form, i.e., in a structural and functional organoid a simple air/CO_2 incubator does not deliver adequate oxygen supply to layered cells. Furthermore, high-density culture cannot be maintained with the limited nutrients available in conventional cultures. For these reasons, construction of a bioreactor that allows 3-dimensional growth in a high-density perfusion culture has been advocated for reconstructing a liver organoid. In our study a radial-flow bioreactor (RFB) developed in Japan was used as a candidate model for high-density perfusion culture. Filled with a porous carrier, this bioreactor permits culture at a cell density 10 times higher than that allowed by a hollow-fiber culture system[5, 6]. Another important point is to select a cell source. Clinically, cells using bio-artificial liver are required to be highly functional and supplied quickly in large quantities. Therefore we established a functional human hepatocellular carcinoma cell line (FLC-5), which can express drug-metabolized enzymes (e.g., human-type carboxyl esterase or cytochrome) and liver-specific proteins such as albumin. *In vitro* this cell line retains its three-dimensional form, developing distinct microvilli on the surface. These cells can be cultured in serum-free ASF104 medium (Ajinomoto, Tokyo). A liver organoid cannot be reconstructed with hepatocytes only. At minimum, coculture of hepatocytes with nonparenchymal cells, such as sinusoidal endothelial cell (SEC) and hepatic stellate cell (HSC) is required. So we established immortalized SEC line M1[7] and an immortalized HSC line A7[8] by isolating nonparenchymal cells from an H-2Kb-tsA58-transgenic mouse liver transfected with the SV40 large T antigen gene[9].

Reconstruction of the liver sinusoid is important for activity of the liver organoid as a functional unit. Also, the open pores on the surfaces of SEC in fenestrae have an important functional role in the liver sinusoid. Fenestrae are the most remarkable characteristics of SEC, as first described by Wisse in 1970[10] using transmission electron microscopy (TEM). Diameters of these pores vary between species, ranging from 100 to 200 nm[11]. These fenestrae facilitate the transport of materials and solutes from the luminal to the abluminal side of the liver parenchymal cells and *vice versa*[12]. The process and mechanism of formation of these pores remain largely unclarified[13, 14]. The presence of actin filaments at the margin of these pores has been demonstrated by electron microscopic studies[15, 16]. Swinholide A, a most potent microfilament-disrupting drug available, has been demonstrated to increase the number of SEC fenestrae[13]. However, when immortalized SEC was treated in a monolayer culture or as a monoculture in the RFB, an increase in number of fenestrae could not be observed when the Swinholide A was introduced. The potential for drug-induced increase also has been reported to disappear in long-term cultures[7].

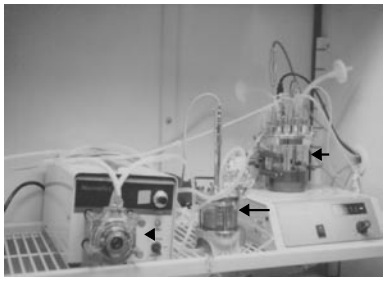

Figure 1 The system of radial-flow bioreactor. A 15-mL radial-flow bioreactor (large arrow), a mass flow controller (arrow head), and a reservoir (small arrow) are connected each other. Culture medium is perfused in the RFB. Medium conditions (PH, oxygen, CO_2 and temperature) are controlled by computer.

In developing a high functioning organoid using a bioartificial liver, the function, form and reactivity of pharmacological agent should be near *in vivo*. In the present study, we reconstructed a functional liver organoid using immortalized cell lines in the RFB.

MATERIALS AND METHODS

Cell culture and medium

We used the three cell lines mentioned above, FLC-5, M1, and A7. As reported, culture of M1 cells was possible in serum-free conditions while supplementation of ASF104 medium with 2% fetal bovine serum (FBS) was required for culture of A7 cells. Therefore, in coculture experiments, ASF104 medium was enriched with 2% FBS.

Coculture in radial-flow bioreactor

As reported elsewhere, the RFB system is composed of a 15-mL radial-flow chamber (RA-15; ABLE, Tokyo), a mass flow controller (RAD925, ABLE), a reservoir (Figure 1), a computer, and a tissue incubator as described previously[17] (Figure 1). The culture medium was oxygenated within the reservoir, and the pH was adjusted automatically to 7.4. Oxygen pressure in the culture medium was measured both within the reservoir and at the outlet of the bioreactor. Relative oxygen consumption was monitored on the basis of the oxygen pressure gradient. During the study the temperature within the reservoir was kept constantly at 37 ℃. Two $\times 10^7$ FLC-5 cells were inoculated into the reservoir. The bioreactor was perfused in a closed circuit for 2 h to aid cells in adhering to the porous carrier cellulose beads (Asahi Kasei, Tokyo). Subsequently the bioreactor was switched to the open-circuit mode, and incubation was continued with addition of fresh culture medium to the reservoir. After 5 d, 2×10^7 A7 cells were added in a similar manner followed by another addition of 10^7 M1 cells 5 d later. Retinol (10^{-6}mol/L) was added during the first 2 d. After three days of perfusion cellulose beads with the adherent cells were harvested, and cells deposited at the bottom of the bioreactor also were recovered. Beads with attached cells were fixed in 1.2% or 2.0% glutaraldehyde as described below.

Swinholide A experiments

We cultured the three cell lines as described above. The

last incubation included perfusion with 200 nmol/L swinholide A (Sigma catalog number S9810; S) for 2 h. The cellulose beads along with adherent cells were harvested from the bioreactor. Beads with attached cells were fixed in glutaraldehyde and prepared for morphologic observation as follows.

Electron microscopy

For scanning electron microscopy (SEM), cultured cells were fixed with 1.2% glutaraldehyde in 0.1 mol/L phosphate buffer (PB) at pH 7.4 and postfixed with 1% OsO_4 in 0.1mol/L PB. The fixed cells were rinsed twice with PBS, subsequently dehydrated in ascending concentrations of ethanol, critical point-dried using carbon dioxide, and coated by vacuum- evaporated carbon and ion-spattered gold. Specimens were observed under JSM-35 scanning electron microscope (JEOL, Tokyo) at an accelerated voltage of 10 kV.

For transmission electron microscopy (TEM), cultured cells were fixed with 2.0% glutaraldehyde in 0.1mol/L PB for 1 h and postfixed with 1% OsO_4 in 0.1mol/L PB for 1 h at 4 ℃. Specimens were dehydrated in ethanol and subsequently embedded in a mixture of Epon-Araldite. Thin sections (60 nm) were cut with a diamond knife mounted on an LKB ultratome, and stained with aqueous uranyl acetate. Specimens were examined under a JEOL 1200EX electron microscope.

Amino acid analysis of supernatants

For analysis of amino acid fractions by high-performance liquid chromatography (HPLC), supernatants were collected from FLC-5 alone and from cocultures of the three cell types in the bioreactor. Supernatants were mixed with 5% sulfosalicylic acid and allowed to stand at 4 ℃ for 15 min. After centrifugation to precipitate protein, supernatants were injected into amino acid analysis columns (L-8500, Hitachi, Tokyo).

Quantitative TaqMan RT-PCR

We measured mRNA expression for the urea cycle enzymes, carbamoyl phosphate synthetase (CPS1), ornithine carbamoyltransferase (OCT), argininosuccinatesynthetase (ASS), argininosuccinatelyase (ASL), and arginase (ARG), as well as mRNA expression for albumin, hepatocyte nuclear factor (HNF)-1 and HNF-4, by quantitative TaqMan reverse transcription polymerase chain reaction (RT-PCR). RT-PCR was performed on the ABI PRISM 7700 sequence detection system using random hexamers from TaqMan reverse transcription reagents and the RT reaction mix (Applied Biosystems, Rockville, M) to reverse-transcribe RNA. TaqMan universal PCR Master Mix and Assays-on-Demand gene expression probes (Applied Biosystems) were used for PCR. A standard curve for serial dilution of 18S rRNAs was generated similarly. A relative standard curve method (Applied Biosystems) was used to calculate the amplification difference in urea cycle-related enzymes between cocultured and control cells, and elongation factor 1 (EF1), for each primer set and between albumin, HNF-1, HNF-4, and glyceraldehyde-3-phosphate dehydrogenase (GAPDH). Specificity was evaluated using GAPDH mRNA as an internal control (4310884E; Perkin-Elmer Applied Biosystems). Each amplification was performed in triplicate, and averages were obtained.

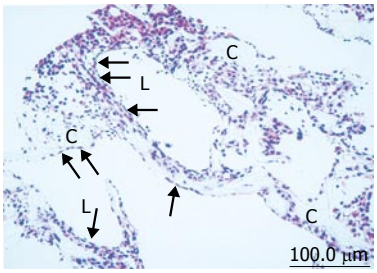

Figure 2 Light microscopic image of coculture in the RFB. High-density and layered cells attached on the cellulose beads (C). Sinusoid-like lumen structure (L) could be observed. SEC was observed with flat shape on surface of the lumen and perfusion side (arrow).

Based on DNA sequences in GenBank, primers and the TaqMan probe for albumin, HNF-1, and HNF-4 were designed using the primer design software Primer Express TM (Perkin-Elmer Applied Biosystems, Foster City, CA). AmpliTaq DNA polymerase extended the primer and displaced the TaqMan probe through its 5'-3' exonuclease activity. Probes were labeled with a reporter fluorescent dye either 6-carboxy-fluorescein (FAM) or 2, 7 dimethoxy-4,5-dichloro-6-carboxy-fluorescein (JOE) at the 5' end and a quencher fluorescent dye [6-carboxytetramethyl-rhodamine (TAMRA)] at the 3' end.

Primers/probes were as follows: ornithine transcarbamoylase (OTC) forward primer 5'-CCAGGCAATAAAAGAGTCAGGATT-3', reverse primer/ 5'-TTATCAAAG TCCCCTGGTTAGAGATACT-3', probe/ 5'-(FAM)- TTCAAATGCTCCTACACCCTGCCCTG-(TAMRA)-3'; arginosuccinase (ASL) forward primer/ 5'-TGGCCAAGGAGGTCGTCA-3', reverse primer 5'-TTCCTCGTCGTCCGGAAG-3', probe 5'-(FAM)-TGTCTTCCAGACCCGGAGACCGAA-(TAMRA)-3'; albumin forward primer/ 5'-CGATTTTCTTTTTAGGGCAGTAGC-3', reverse primer/ 5'-TGGAAACTTCTGCAAACTCAGC-3', probe/ 5'-(FAM)-CGCCTGAGCCAGAGATTTCCCA-(TAMRA)-3'; HNF-1 forward primer/ 5'-AGCGGGAGGTGGTCGATAC-3', reverse primer/ 5'-CATGGGAGTGCCCTTGTTG-3', probe/ 5'-(FAM)-TCAACCAGTCCCACCTGTCCCAACA-(TAMRA)-3'; HNF-4 forward primer/ 5'-GGTGTCCATACGCATCCTTGA-3', reverse primer/ 5'-TGGCTTTGAGGTAGGCATACTCA-3', probe/ 5'-(FAM)-CCTTCCAGGAGCTGCAGATCGATGAC-(TAMRA)-3'; GAPDH forward primer/ 5'-CTCCCCACACACATGCACTTA-3', reverse primer/ 5'-CCTAGTCCCAGGGCTTTGATT-3', probe/ 5'-(VIC)-AAAAGAGCTAGGAAGGACAGGCAACTTGGC-(TAMRA)-3'.

RESULTS

Structure of cells cultured in bioreactor

In the bioreactor, cells cultured in high density assumed layered form on the cellulose beads. Lumen-like structure was observed. Endothelial cells were exits with flat shape at the surface of the lumen and the perfusion side (Figure 2). Multiple layers of FLC-5 cells adhered to the cellulose beads, while A7 and M1 cells were predominantly localized to the side where perfusion occurred. Layered cells were seen in a hole of porous cellulose beads. Sinusoid-like lumen was observed at perfusion side in the cellulose beads

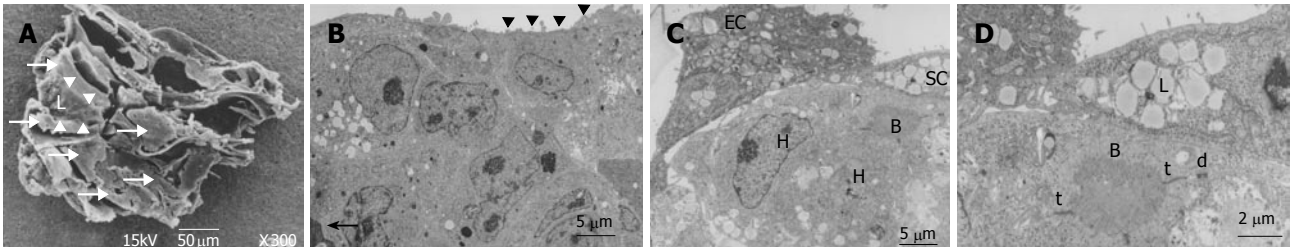

Figure 3 Transmission electron microscopic images of cocultures in the RFB. **A**: The cells are arrayed on the cellulose beads. Several cell clusters could be seen in a gap of cellulose beads (arrow). Vascular lumen structure surrounding cell clusters could be seen in the beads (small arrow). Culture media flow through inside of lumen structure; **B**: The cells are arrayed in layers on cellulose beads. Part of a cellulose bead (arrow) is visible at the bottom of the layer. A process of a sinusoidal endothelial cell (arrowhead) is seen at the perfusion side. Scale bar: 5 μm; **C**: Sinusoidal endothelial cells (EC) can be seen at the perfusion side. Hepatic stellate cells (SC) containing fatty vitamin A droplets are seen overlying the FLC-5 cells (H). FLC-5 cells (H) below EC and SC show bile-canaliculus-like structures (B). Scale bar: 5 μm. **D**: Bile canaliculus-like structures (B) containing electron dense bile components. Tight junctions (t) and desmosomes (d) are visible, as are fatty vitamin A droplets (L). Scale bar: 2 μm.

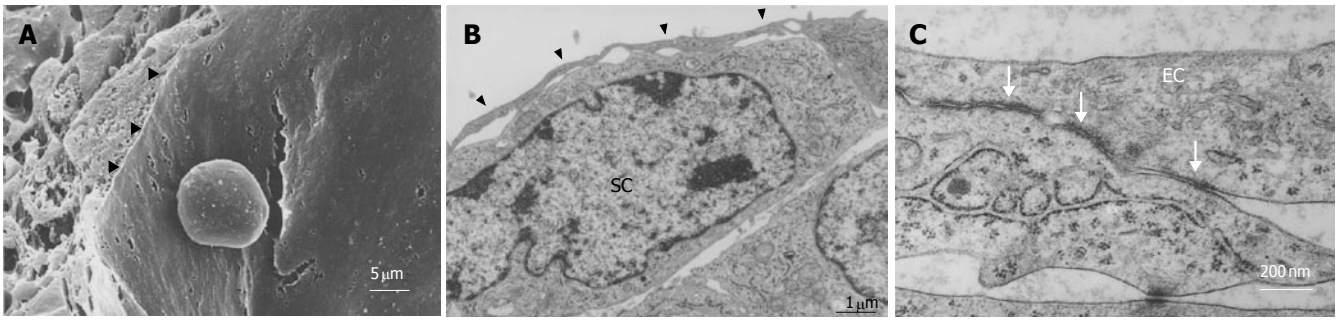

Figure 4 Ultrastructure of sinusoidal endothelial cells. **A**: Scanning electron microscopic image of sinusoidal endothelial cells localized at the perfusion side. They form a thin layer (arrowhead), showing the typical appearance of a sinusoid-like vascular structure. Scale bar: 5 μm; **B**: Transmission electron microscopic image showing sinusoidal endothelial cell growth at the perfusion side forming a thin layer (arrowhead) overlying the A7 cells (SC). Scale bar: 1 μm; **C**: Transmission electron microscopic view showing tight junctions (arrow) between sinusoidal endothelial cells (EC). Scale bar: 200 nm.

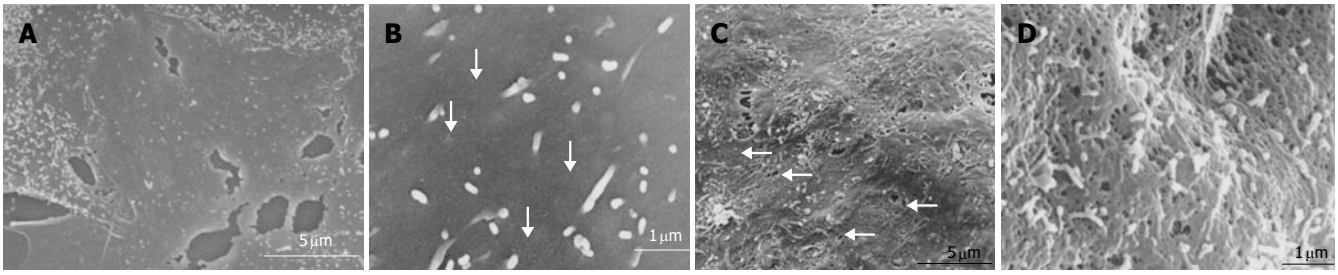

Figure 5 Scanning electron microscopic image of the surface of sinusoidal endothelial cells. **A**: Low-magnification scanning electron microscopic images of the surface of sinusoidal endothelial cells cultured on plastic dishes. The sinusoidal endothelial cells formed a thin layer on the plastic dish substrate. Scale bar: 5 μm; **B**: High-magnification scanning electron microscopy images of the surface of sinusoidal endothelial cells cultured on plastic dishes. Fenestrae could not be detected on the surface of endothelial cells. Only small pits are seen (arrow). Scale bar: 1 μm; **C**: Low-magnification scanning electron microscopic view of the surface of sinusoidal endothelial cells cocultured in the RFB. Fenestrated pores could be observed (arrow). Scale bar: 5 μm; **D**: High-magnification scanning electron microscopic view of the surface of sinusoidal endothelial cells cocultured in the RFB. Pores have a diameter of 100 - 200 nm. Scale bar: 1 μm.

(Figure 3A). TEM showed that cocultured cells assumed layered form from cellulose beads to the perfusion side (Figure 3B). M1 and A7 cells containing vitamin A-laden fat droplets were seen mainly at the perfusion side, while dense layers of FLC-5 cells were observed beneath (Figure 3C). At sites where the three cell lines were in contact with each other bile canaliculus-like structures were present between neighboring FLC-5 cells. Lumens of these structures contained electron-dense bile components, tight junctions and desmosomes also could be observed (Figure 3D). This side showed growth of endothelial cells with the formation of sinusoid-like vascular structures (Figures 4A and 4B). Tight junctions were seen between endothelial cells (Figure 4C). Fenestrae which are characteristic of SEC *in vivo*, were absent in monocultures of M1 cells on plastic dishes (Figures 5A and 5B). Because a long time subculture would change the character of M1 cells, pores were represent on the surface of M1 cells co-cultured in the RFB system (Figure 5C). The pores had a diameter of 100 to 200 nm, being similar in morphology and size to those of fenestrae shown by SEC *in vivo* (Figure 5D).

Morphology of M1 cells incubated with swinholide A

Cells incubated for 2 h with 200 nmol/L of the actin-disrupting agent swinholide A showed the increased number of pores (Figure 6), while some pores were dilated (about

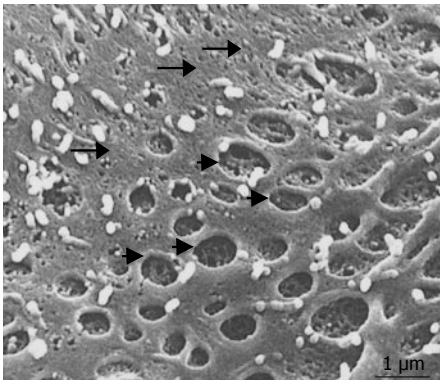

Figure 6 Scanning electron micrographs of the surface of swinholide A - treated SEC cells in the RFB culture system. Large open pores have a fenestra-like appearance (short arrow). Small pores were detectable in the nonfenestrated area (long arrow). Scale bar: 1 μm.

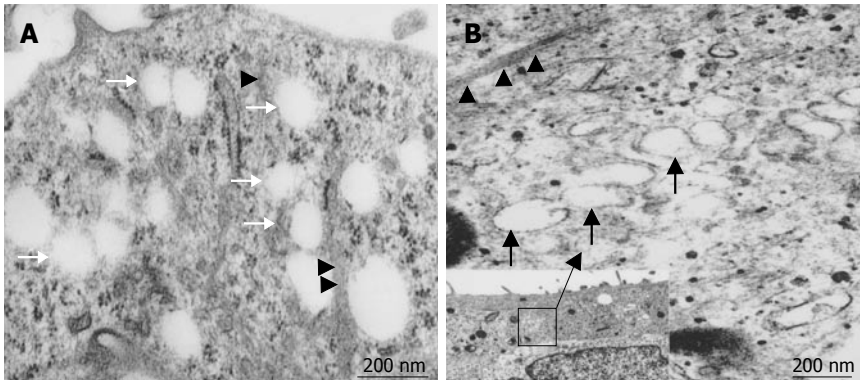

Figure 7 Transmission electron micrographs of sectioned SEC cells after swinholide A - treatment; **A**: Numerous open pores or fenestrae in the cytoplasm (arrow). Fine cytoskeletal elements showing a close spatial relationship with these pores (arrowhead). Scale bar: 200 nm; **B**: VVO could be observed in SEC cells (arrows) in response to stress or actin fibers (arrowheads). Scale bar: 200 nm. Inset shows the overall composition of the cells. Scale bar: 1 μm.

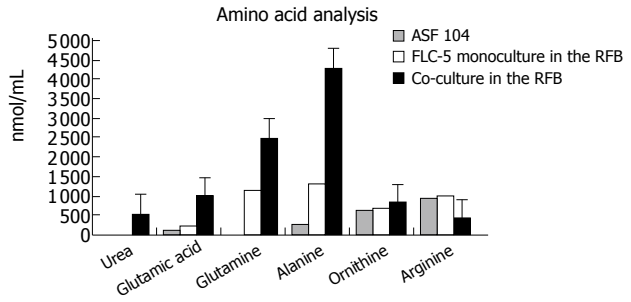

Figure 8 Amino acid and urea analysis in supernatants. Urea was detectable only in coculture, at 523 nmol/ml. ASF 104 designates culture medium. Mean value ± SD.

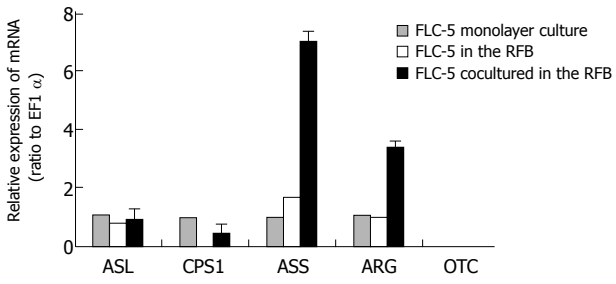

Figure 9 Comparison of expressions of CPS1, OTC, ASS, ASL, and ARG mRNA in FLC-5 incubated under different conditions as assessed by TaqMan 1-step RT-PCR. The mRNA expression of each enzyme in different conditions is relative to that in monolayer cultures. Mean value ± SD.

1 μm). Small pores (tens of nanometers in size) that probably resembled coated pits were abundant in the nonfenestrated areas.

TEM investigation showed that treatment with swinholide A resulted in fenestrated pores with a diameter between 100 and 200 nm. The pores fused with each other formed labyrinthine structures (Figure 7A). In addition, vacuoles with a diameter of about 200 nm, similar to previously described vesiculo vacuolar organelles (VVO), were noted. These structures typically were seen in areas where relatively regular overlap was seen in FLC-5, A7, and M1. The number of VVO increased when cells were treated with 200 nmol/L swinholide A, which was associated with partial fusion (Figure 7B).

Amino acid fractions from supernatants

At the end of culture, the supernatant was subjected to amino acid analysis. Urea production was not seen in monocultures of FLC-5 cells in the RFB, while FLC-5 cells cocultured with M1 and A7 cells produced 523 nmol urea /mL in the culture medium, suggesting that the urea cycle was activated in the coculture RFB system (Figure 8). Several amino acids were increased in the medium.

We compared mRNA expression of CPS1, OTC, ASS, ASL, and ARG in FLC-5 monolayer cultures with those of monocultures in the RFB system. In addition, mRNA expression in cocultures in the RFB also was assessed. We could not detect OTC in any type of culture. Expression of other urea cycle enzymes showed no notable difference between monolayer culture of FLC-5 and monoculture of FLC-5 in the RFB. However, ASS and ARG expressions in co-culture in the RFB were about 7 and 3 times greater than those in FLC-5 monolayer culture (Figure 9).

Albumin synthesis and expression of nuclear factors

We compared mRNA expression of albumin and HNF-1 and HNF-4 as transcription regulation factors between experimental conditions. Expression of mRNA encoding the three proteins was less in FLC-5 co-cultures in the RFB system than in FLC-5 RFB monocultures or in FLC-5 cells in monolayer culture (Figures 10A-10C). In a previous study, albumin production was enhanced in the RFB using the immortalized cell line[17]. However it was different cell line in this study.

DISCUSSION

Introduction of a functional human hepatocellular carcinoma cell line (FLC) in our system can allow the cells to be cultured at high density in a layered array and maintain viability for long periods[17,18].

Immortalized cells can be used for artificial liver. The reason is that it can supply cells in large quantities and quickly. Immortalized cells lose several characteristics in

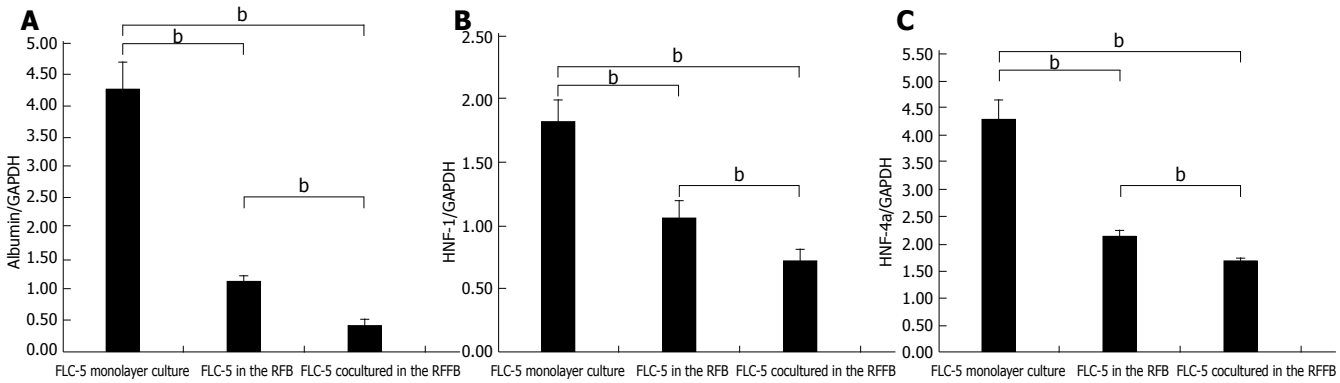

Figure 10 Expression of mRNA for albumin (**A**), HNF-4 (**B**) and HNF-1 (**C**) as transcription regulation factors in each condition. Messenger RNA expression for these three proteins decreased in cocultured FLC-5 in the RFB compared with FLC-5 monocultures in the RFB and FLC-5 cultured in a monolayer. Mean value ± SD. The ratio of mRNA for each protein versus GAPDH is shown. Differences with respect to each condition were statistically significant ($^bP < 0.01$) according to Student's *t*-test.

morphology and function. However, three cell lines were studied in our RFB culture system, including their fine structure according to electron microscopy. Layers of FLC-5, A7, and M1 were arranged respectively from the carrier attachment side to the perfusion side. In some areas, liver-like architectures, sinusoid-like lumen structure, bile-canaliculi and functional complex, were observed, comparable to *in vivo* tissue relationship. The M1 cell line well covered the perfusion side, mimicking vascular structures, indicating that this cell type forms an arrangement similar to that *in vivo*. Furthermore, M1 cells in monolayer culture did not express fenestrae, probably reflecting a long culture or subculture time[19]. In a previous study, we found that M1 cells also lack fenestrae in monocultures in the RFB[7]. In contrasts, fenestrated pores were seen in M1 cells cocultured according to the present RFB experimental design. Coculture and cell to cell contact have an influence on these morphological changes. Because fine structures *in vivo* could be observed better than monoculture in the RFB.

The electron microscopic observations in the present study clearly showed that if an appropriate environment for cell growth was provided in a perfusion culture system, the individual cell types could arrange themselves according to their *in vivo* characteristics, even in a high-density layered culture.

This study also examined the numerical dynamics of fenestrae. For this we exposed the cocultures to the actin-disrupting drug swinholide A[13]. When the cells were treated with swinholide A, the number of pores with a diameter of about 100 to 200 nm increased 2 h after swinholide A treatment. Furthermore, by TEM, cytoplasmic vesicles about 200 nm in diameter could be seen and were much larger than the caveolae in the cytoplasm, and their number increased in the presence of swinholide A. These vacuolar-like vesicles probably represent the vesiculo vacuolar organelle (VVO) as described by Feng *et al*[20]. The VVO is an organelle contributing to transport of macromolecules between luminal and abluminal sides of endothelial cells, thus increasing transcellular permeability. Vascular permeability factor and vascular endothelial growth factor (VPF/VEGF) can induce formation of VVO[21]. FLC-5 used in this study, could express VPF/VEGF (data not shown). The presence of vascular factors may partially explain why VVO is noted in cocultures and why fenestrae could be observed in our experiments[22]. VVO is thought to be formed by fusion of caveolae, when multiple VVOs fuse together, a structure extending from the luminal to the abluminal sides of endothelial cells is formed. In the present study, fused VVOs also were seen in swinholide A - treated specimens by transmission electron microscopy, suggesting that this fusion represents a process culminating in formation of the labyrinthine structures in SEC[23]. The mechanism of pore formation in immortalized SEC and under cocultured perfusion conditions remains unknown from the present study. However, pore formation may result from multiple effects or factors working in concert upon endothelial cells, such as cytoskeletal dynamics represented by actin and/or the influence of a yet unknown factor secreted by other cell types present in the cocultures such as VEGF. The observation that hepatic endothelial cells maintain one of their typical morphological features (i.e. an abundant number of membrane-bound coated-pits, uncoated vesicles/vacuoles and fenestrae) is an indication that the bioreactor mimics a nearby physiological cultivation environment for the various liver cell types. However, the mechanism by which the bioreactor and its culture environment bring about and maintain these membrane-bound vesicles and fenestrae in endothelial cells remain to be elucidated and consequently open up new directions for future experiments.

To assess hepatocyte function, we compared mRNA expression for urea cycle enzymes and albumin synthesis by FLC-5 in monolayer culture compared to these single-type cultures and cocultures in the RFB. Previously, we have demonstrated hepatocyte functions such as albumin synthesis and cytochrome expression are enhanced in the RFB[24, 25]. Urea production is among the most primitive functions of liver cells. We could not detect urea in medium from monolayer cultures or monocultured FLC-5 in the RFB. In contrast, FLC-5 cells cocultured in the RFB exhibit ability to produce urea, and mRNA expression for ASS and ARG is enhanced. The medium used in this experiment, ASF 104 contained arginine, so urea production was observed in cocultures in the RFB although OTC was not expressed. One report showed that urea produc-

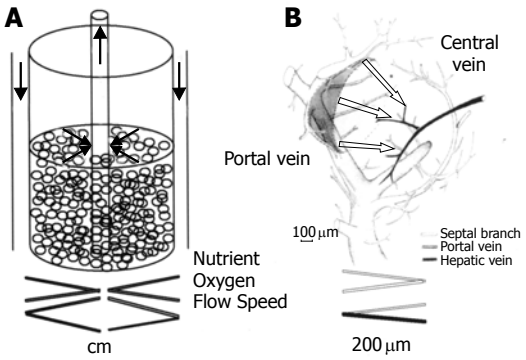

Figure 11 RFB and intact organ. **A**: In the RFB system, culture medium flows from outside the column toward the center of the reactor. Medium flows faster at the center than at the periphery. Biases in distribution of oxygen and nutrition at inflow and outflow are minimized. **B**: In the hepatic lobe, blood flows from the portal vein to central vein. The RFB system is similar to the organization of the hepatic primary lobe[31]. Figure 11B is reproduced from Figure 9 in reference 31.

tion in OTC-deficient mice could be detected under the same condition[26]. Glutamic acid, glutamine and alanine were also increased in supernatant co-cultured in the RFB, indicating that amino acid metabolism becomes active.

It was reported that three-dimensional spherical culture induces albumin synthesis, a particularly important hepatocytic function[27, 28]. However, in the present study, mRNA expression of albumin was decreased under coculture conditions in the RFB. Nuclear transcriptional factors HNF-4 and HNF-1, which regulate albumin synthesis, were decreased under coculture conditions in the RFB. Albumin in supernatant was also decreased during culture (data not shown). The results suggest that the culture environment (cell-to-cell communication, cell polarity, shear stress, and other factors) can control manifestations of intracellular nuclear transcription factors and therefore dramatically influence albumin production by liver cells. Immortalized cells can be used for artificial liver. The reason is that it can supply cells in large quantities and quickly. But immortalized cells may change the characteristics of its original cells. In this study, albumin synthesis was decreased. It was not useful for artificial liver. In future study, we have to try other cell sources (ES cell, oval cell, and other immortalized cell lines).

Finally, several points should be noted concerning our culture system. First, controlling the mixture ratio of the three cell types used is very difficult since each type possesses its own potential for active growth. Thus, growth rates vary between cell types and are difficult to control. For examples, A7 cells grew less rapidly and tended to be less than the other two cell types in the coculture system. Second, the hepatic lobule spans about 140 μm *in vivo*, extending from the portal to the central area, toward which portal blood flows in a radial manner. According to Matsumoto *et al*[29], the liver is an organ composed of numerous groups of microscopic three-dimensional units (minimal radial-flow bioreactors) extending from the inflow side (composed of combinations of parabola-shaped inflow fronts) to the central vein[30]. According to this model, the liver microcirculation as observed *in vivo* could not be reproduced faithfully with a radial-flow bioreactor, since the distance between inflow and outflow sides in the bioreactor is about 1.5 cm (Figure 11). Third, bile canaliculus-like structures are formed between hepatocytes. Since we did not use the bile duct cells in this study, whether different cell types can reconstruct bile ducts remains to be elucidated[31]. Finally, although several questions remain, the results of the present study suggest that liver reconstruction is possible *in vitro*. Such organ reconstruction technology is expected to contribute greatly to the development of sophisticated artificial livers and other organs for transplantation. Our culture system may be a very important tool to maintain liver organ.

ACKNOWLEDGMENTS

The authors thank Mr. Hideki Saito, Mrs. Emi Kikuchi, and Mrs. Hisako Arai of the DNA Medical Institute at The Jikei University School of Medicine for technical assistance with electron microscopy. The authors also thank the members of the Australian Key Center for Microscopy and Microanalysis of The University of Sydney for their excellent administrative, technical, and practical support.

REFERENCES

1 **Gordon GJ,** Butz GM, Grisham JW, Coleman WB. Isolation, short-term culture, and transplantation of small hepatocyte-like progenitor cells from retrorsine-exposed rats. *Transplantation* 2002; **73**: 1236-1243
2 **Kanda T**, Watanabe S, Yoshiike K. Immortalization of primary rat cells by human papillomavirus type 16 subgenomic DNA fragments controlled by the SV40 promoter. *Virology* 1988; **165**: 321-325
3 **Nishida K,** Yamato M, Hayashida Y, Watanabe K, Yamamoto K, Adachi E, Nagai S, Kikuchi A, Maeda N, Watanabe H, Okano T, Tano Y. Corneal reconstruction with tissue-engineered cell sheets composed of autologous oral mucosal epithelium. *N Engl J Med* 2004; **351**: 1187-1196
4 **Tabata Y.** Tissue regeneration based on growth factor release. *Tissue Eng* 2003; **9 Suppl 1**: S5-S15
5 **Sussman NL,** Chong MG, Koussayer T, He DE, Shang TA, Whisennand HH, Kelly JH. Reversal of fulminant hepatic failure using an extracorporeal liver assist device. *Hepatology* 1992; **16**: 60-65
6 **Sussman NL,** Kelly JH. Improved liver function following treatment with an extracorporeal liver assist device. *Artif Organs* 1993; **17**: 27-30
7 **Matsuura T,** Kawada M, Hasumura S, Nagamori S, Obata T, Yamaguchi M, Hataba Y, Tanaka H, Shimizu H, Unemura Y, Nonaka K, Iwaki T, Kojima S, Aizaki H, Mizutani S, Ikenaga H. High density culture of immortalized liver endothelial cells in the radial-flow bioreactor in the development of an artificial liver. *Int J Artif Organs* 1998; **21**: 229-234
8 **Matsuura T**, Kawada M, Sujino H, Hasumura S, Nagamori S, Shimizu H. Vitamin A metabolism of immortalized hepatic stellate cell in the bioreactor. In: Wisse E, Knook D L, De Zanger R, Arthur M J P, eds. Cells of the Hepatic Sinusoid 7. Leiden: *Kupffer Cell Foundation*, 1999: 88-89
9 **Jat PS**, Noble MD, Ataliotis P, Tanaka Y, Yannoutsos N, Larsen L, Kioussis D. Direct derivation of conditionally immortal cell lines from an H-2Kb-tsA58 transgenic mouse. *Proc Natl Acad Sci U S A* 1991; **88**: 5096-5100
10 **Wisse E**. An electron microscopic study of the fenestrated endothelial lining of rat liver sinusoids. *J Ultrastruct Res* 1970; **31**: 125-150
11 **Braet F.** How molecular microscopy revealed new insights into the dynamics of hepatic endothelial fenestrae in the past

decade. *Liver Int* 2004; **24**: 532-539
12 **Fraser R**, Dobbs BR, Rogers GW. Lipoproteins and the liver sieve: the role of the fenestrated sinusoidal endothelium in lipoprotein metabolism, atherosclerosis, and cirrhosis. *Hepatology* 1995; **21**: 863-874
13 **Braet F**, Spector I, De Zanger R, Wisse E. A novel structure involved in the formation of liver endothelial cell fenestrae revealed by using the actin inhibitor misakinolide. *Proc Natl Acad Sci U S A* 1998; **95**: 13635-13640
14 **Braet F,** Spector I, Shochet N, Crews P, Higa T, Menu E, de Zanger R, Wisse E. The new anti-actin agent dihydrohalichondramide reveals fenestrae-forming centers in hepatic endothelial cells. *BMC Cell Biol* 2002; **3**: 7
15 **Oda M**, Tsukada N, Komatsu H, Kaneko K, Nakamura M, Tsuchiya M: Electron microscopic localizations of actin, calmodulin and calcium in the hepatic sinusoidal endothelium in the rat. In: Kirn A, Knook DL, Wisse E des. Cells of the Hepatic Sinusoid 1. Rijswijk, *Kupffer Cell Foundation* 1986; 511-512
16 **Gatmaitan Z**, Varticovski L, Ling L, Mikkelsen R, Steffan AM, Arias IM. Studies on fenestral contraction in rat liver endothelial cells in culture. *Am J Pathol* 1996; **148**: 2027-2041
17 **Kawada M,** Nagamori S, Aizaki H, Fukaya K, Niiya M, Matsuura T, Sujino H, Hasumura S, Yashida H, Mizutani S, Ikenaga H. Massive culture of human liver cancer cells in a newly developed radial flow bioreactor system: ultrafine structure of functionally enhanced hepatocarcinoma cell lines. *In Vitro Cell Dev Biol Anim* 1998; **34**: 109-115
18 **Aizaki H**, Nagamori S, Matsuda M, Kawakami H, Hashimoto O, Ishiko H, Kawada M, Matsuura T, Hasumura S, Matsuura Y, Suzuki T, Miyamura T. Production and release of infectious hepatitis C virus from human liver cell cultures in the three-dimensional radial-flow bioreactor. *Virology* 2003; **314**: 16-25
19 **Braet F,** de Zanger R, Seynaeve C, Baekeland M, Wisse E. A comparative atomic force microscopy study on living skin fibroblasts and liver endothelial cells. *J Electron Microsc (Tokyo)* 2001; **50**: 283-290
20 **Feng D,** Nagy JA, Hipp J, Dvorak HF, Dvorak AM. Vesiculovacuolar organelles and the regulation of venule permeability to macromolecules by vascular permeability factor, histamine, and serotonin. *J Exp Med* 1996; **183**: 1981-1986
21 **Feng D**, Nagy JA, Pyne K, Hammel I, Dvorak HF, Dvorak AM. Pathways of macromolecular extravasation across microvascular endothelium in response to VPF/VEGF and other vasoactive mediators. *Microcirculation* 1999; **6**: 23-44
22 **Yokomori H**, Oda M, Yoshimura K, Nagai T, Ogi M, Nomura M, Ishii H. Vascular endothelial growth factor increases fenestral permeability in hepatic sinusoidal endothelial cells. *Liver Int* 2003; **23**: 467-475
23 **Oda M**, Yokomori H, Han J Y, Kamegaya Y, Ogi M, Nakamura M. Hepatic sinusoidal endothelial fenestrae are a stationary type of fused and interconnected caveolae. In: Wisse E, Knook D L, De Zanger R, Arthur M J P, eds. Cells of the Hepatic Sinusoid 8. Leiden: *Kupffer Cell Foundation*, 2001: 94-98
24 **Nagamori S,** Hasumura S, Matsuura T, Aizaki H, Kawada M. Developments in bioartificial liver research: concepts, performance, and applications. *J Gastroenterol* 2000; **35**: 493-503
25 **Iwahori T,** Matsuura T, Maehashi H, Sugo K, Saito M, Hosokawa M, Chiba K, Masaki T, Aizaki H, Ohkawa K, Suzuki T. CYP3A4 inducible model for in vitro analysis of human drug metabolism using a bioartificial liver. *Hepatology* 2003; **37**: 665-673
26 **Li MX,** Nakajima T, Fukushige T, Kobayashi K, Seiler N, Saheki T. Aberrations of ammonia metabolism in ornithine carbamoyltransferase-deficient spf-ash mice and their prevention by treatment with urea cycle intermediate amino acids and an ornithine aminotransferase inactivator. *Biochim Biophys Acta* 1999; **1455**: 1-11
27 **Glicklis R**, Merchuk JC, Cohen S. Modeling mass transfer in hepatocyte spheroids via cell viability, spheroid size, and hepatocellular functions. *Biotechnol Bioeng* 2004; **86**: 672-680
28 **Ma M**, Xu J, Purcell WM. Biochemical and functional changes of rat liver spheroids during spheroid formation and maintenance in culture: I. morphological maturation and kinetic changes of energy metabolism, albumin synthesis, and activities of some enzymes. *J Cell Biochem* 2003; **90**: 1166-1175
29 **MacSween R**. N. M. Pathology of the Liver, 4th ed. In: Developmental anatomy and normal structure, *Churchill Livingstone*, 2002: 16-22
30 **Matsumoto T**, Komori R, Magara T, Ui T, Kawakami M, Hano H. A study on the normal structure of the human liver, with special reference to its angioarchitecture. *Jikei Med J* 1979; **26**: 1-40
31 **Ishida Y,** Smith S, Wallace L, Sadamoto T, Okamoto M, Auth M, Strazzabosco M, Fabris L, Medina J, Prieto J, Strain A, Neuberger J, Joplin R. Ductular morphogenesis and functional polarization of normal human biliary epithelial cells in three-dimensional culture. *J Hepatol* 2001; **35**: 2-9

S- Editor Wang J **L- Editor** Wang XL **E- Editor** Liu WF